# Self-Diffusion in Branched Polymer Melts

**Craig R. Bartels[1] and Buckley Crist, Jr.**

*Materials Science and Engineering Department, Northwestern University, Evanston, Illinois 60201*

**Lewis J. Fetters and William W. Graessley***

*Corporate Research—Science Laboratories, Exxon Research and Engineering Company, Annandale, New Jersey 08801.* *Received August 1, 1985*

ABSTRACT: The self-diffusion coefficient $D$ and zero-shear viscosity $\eta_0$ were measured in the melt state for a series of three-arm star hydrogenated polybutadienes. Values of $D$ were obtained by the layered film/small-angle neutron scattering technique that had been used earlier for melts of linear hydrogenated polybutadiene. Both $D$ and $\eta_0$ depend exponentially on arm molecular weight $M_a$, and their product $\eta_0 D$ is proportional to $M_a^{-1}$, as predicted by simple arguments based on the tube model. Self-diffusion was found to be much faster than tracer diffusion in a high molecular weight matrix, suggesting a large contribution to both star polymer mobility and viscoelasticity from the finite lifetime of tube constraints. A model that includes that contribution seems to accommodate both linear and branched polymer results fairly well.

## Introduction

Diffusion data in the melt state have been reported recently for entangled polymers of several species.[2-10] Various techniques were used to obtain the tracer diffusion coefficient, where the diffusant polymer is present at low concentration in a matrix of the same species but different molecular weight, or the self-diffusion coefficient, where diffusant and matrix are identical or differ only by isotopic substitution. Most results for highly entangled *linear* polymers seem consistent with the following interpretation. The diffusant moves by two independent processes—reptation at a rate that is independent of the matrix molecular weight, and constraint release (tube renewal) at a rate that is governed by the reptation of matrix chains. The constraint release contribution becomes less important for longer chains, and, unless the diffusant is much larger than the matrix chains, diffusant reptation eventually dominates. Tracer and self-diffusion coefficients are then equal, and the reptation law for a fixed matrix applies

$$D_L = k_D M^{-2} \tag{1}$$

where $M$ is the diffusant molecular weight. Theories of dynamics based on the reptation model provide reasonable estimates of $k_D$ from viscoelastic data.[11,12] Computer simulations of tracer diffusion in a fixed matrix give an $M^{-2}$ dependence.[13] Simulations of self-diffusion are less conclusive,[14-16] but the data suggest an approach to $M^{-2}$ behavior near the upper limit set by current computer capacities.[17]

Diffusion data for entangled *branched* polymers are only now becoming available.[3,5] Long branches would be expected to suppress reptation, so mechanisms that are too slow to affect the mobility of linear diffusants might now become important. The contributions of constraint release also need reevaluation. de Gennes has suggested that the rate-limiting step for diffusion of star polymers in a fixed matrix is the formation of nonentangled configurations by the arms.[18] Such a configuration would be formed if the end of a branch exactly retraces its path back to the branch point so that no matrix chains are enclosed in the loop. From considerations about the probability of such "retracted" states, he proposed an exponential law for three-arm stars

$$D_B = A_1 \exp(-A_2 M_a) \tag{2}$$

where $M_a$ is the molecular weight of the arm. The prefactor $A_1$ may contain some power of $M_a$ as well. This form is consistent with computer simulations for three-arm stars in a fixed matrix[19] and with tracer diffusion data for three-arm stars of hydrogenated polybutadiene in a matrix of high molecular weight polyethylene.[3] Some indirect support comes also from the observed exponential dependence of melt viscosity on $M_a$ for star polymers.[20,21]

The work reported here supplements those data with self-diffusion coefficients for melts of three-arm star hydrogenated polybutadiene (HPB). The values were obtained from the rate of homogenization of layered films, a method used recently to study self-diffusion in melts of linear HPB.[10] The results, together with viscoelastic measurements and the HPB tracer diffusion data,[3] are used to explore the role of matrix in the dynamic properties of entangled stars. The self-diffusion data presented here extend to much larger branch lengths than covered in previous work. In the following section we attempt to unify theory, simulation results, and experimental data for fixed matrix diffusion to provide an extrapolation formula for comparison with our self-diffusion results at higher molecular weights. The outcome is somewhat inconclusive insofar as extrapolation is concerned, but such comparisons are of general interest so we include them.

## Preliminary Considerations

Theoretical predictions and data about the mobility of entangled stars come from several sources and have been reported in different ways. To simplify comparisons among the various results we have reduced them to a common basis, using some equations from the Doi–Edwards theory[11,12,22] when necessary. Arm length is expressed in entanglement units $M_a/M_e$, where $M_e$ is the entanglement molecular weight[23]

$$M_e = \rho RT/G_N^0 \tag{3}$$

in which $G_N^0$ is the plateau modulus, $\rho$ is the melt density, $R$ is the universal gas constant, and $T$ is the temperature. Diffusion coefficients for three-arm stars and linear chains with $M = M_a$ are compared for the same matrix and local dynamics. Results are given as $D_B/D_L$ vs. $M_a/M_e$ which we expect to be universal for sufficiently entangled polymers in a fixed matrix.

**Diffusion of Stars in a Fixed Matrix.** The arm retraction mechanism leads to the following expression for the diffusion coefficient of three-arm stars in a fixed matrix.[22]

$$D_B = \Gamma a^2 P_0/2(\tau_e)_B \tag{4}$$

where $a$ is the mesh size of the matrix, $(\tau_e)_B$ is the equil-

0024-9297/86/2219-0785$01.50/0 

ibration time for an arm, and $P_0$ is the fraction of fully retracted arms, i.e., arms with zero primitive path length.[11] The branch point is assumed to jump randomly to an adjacent matrix position each time one of the arms assumes a fully retracted configuration. The factor $\Gamma$ is included to absorb dynamical effects that are difficult to quantify in general terms—contributions from fluctuations in the branch point location,[3] from the requirement that the initial direction for the new path of a retracted arm be along one of the other arms,[19] and from conformational memory, tending to bias the retracted arm to move back along its direction of original approach.

The distribution of primitive path lengths has been calculated for $N_0$-step random walks on the centers of a regular lattice of uncrossable lines.[19,24] For $N_0 \gg 1$ and $q \geq 3$, the fraction with zero length, i.e., that return to the origin without enclosing any lines, is[24]

$$P_0(N_0) = \frac{4}{(2\pi)^{1/2}} \frac{q(q-1)}{(q-2)^2} N_0^{-3/2} \exp\left[-\frac{N_0}{2} \ln \frac{q^2}{4(q-1)}\right] \quad (5)$$

where $q$ is the number of choices for the step directions ($q = 6$ for a cubic lattice). The average number of the primitive path steps for all walks ($N_0 \gg 1$) is[24]

$$N = \left(\frac{q-2}{q}\right) N_0 \quad (6)$$

and, according to the Doi–Edwards theory[22]

$$N = {}^5/_4 (M_a/M_e) \quad (7)$$

The number of chain steps $N_0$ is eq 5 can therefore be eliminated in favor of $M_a/M_e$

$$N_0 = \frac{5}{4}\left(\frac{q}{q-2}\right) \frac{M_a}{M_e} \quad (8)$$

To eliminate $a^2/(\tau_e)_B$ in eq 4 we use the following Doi–Edwards expression for the diffusion coefficient of linear chains

$$D_L = \frac{a^2}{18\pi^2(\tau_e)_L} \quad (9)$$

Taking $(\tau_e)_L = (\tau_e)_B/4$ to be the equilibration time for linear chains with $M = M_a$,[22] we obtain

$$a^2/(\tau_e)_B = (9\pi^2/2)D_L \quad (10)$$

When those substitutions are made in eq 4, we obtain, for a cubic lattice ($q = 6$) and large $M_a/M_e$

$$D_B/D_L = 25.9\Gamma(M_a/M_e)^{-3/2} \exp[-0.55M_a/M_e] \quad (11)$$

Only the exponential coefficient ($\gamma(q) = 0.55$ for $q = 6$) changes significantly with $q$. For arbitrary $q$

$$\gamma(q) = \frac{5}{8}\left(\frac{q}{q-2}\right) \ln\left[\frac{q^2}{4(q-1)}\right] \quad (12)$$

The computer simulation results for diffusion in a cubic line lattice ($q = 6$) can be reduced in a similar fashion. The static picture is the same: chains are represented as random walks on the lattice centers (step size equals lattice spacing). The dynamics are introduced as random local moves, subject to certain rules that forbid the crossing of lattice lines. Data were obtained for linear chains[13] ($5 \leq N_0 \leq 50$) and three-arm stars[19] ($3 \leq (N_0)_a \leq 15$, where $(N_0)_a = N_0/3$), with and without uncrossability restrictions. Reported values have been arbitrarily divided by 6 to correspond to the conventional definition for a diffusion coefficient. For linear chains

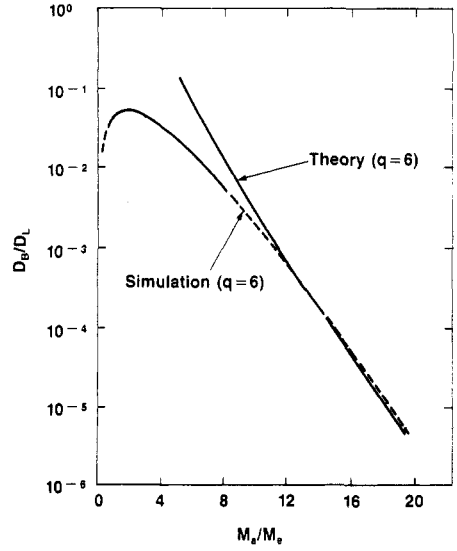


**Figure 1.** Comparison of theory and computer simulation for diffusion through a fixed cubic lattice. Theory (eq 11 with $\Gamma = 1$) and computer data (eq 18) over the simulation range are shown by solid lines. The dashed line is a continuation of eq 18.

$$D_L = 0.16N_0^{-2} \quad (13)$$

$$D_L^* = 0.317N_0^{-1} \quad (14)$$

where $D_L^*$ refers to the result without uncrossibility restrictions and corresponds to the Rouse diffusion coefficient in the computer time scale. According to Doi and Edwards[11]

$$D_L = D_L^*/3N \quad (15)$$

giving (from eq 13 and 14)

$$N = 0.66N_0 \quad (16)$$

This result is in excellent agreement with the analytical prediction of $N = (2/3)N_0$ for the cubic lattice ($q = 6$ in eq 6). The least-squares fit of the data from computer simulation of three-arm star diffusion[19]

$$D_B = 0.0055(N_0)_a^{-0.59} \exp[-0.37(N_0)_a] \quad (17)$$

when combined with eq 13 and $(N_0)_a = 1.89M_a/M_e$ (from eq 8), gives

$$D_B/D_L = 0.085(M_a/M_e)^{1.41} \exp[-0.70M_a/M_e] \quad (18)$$

for the star polymer simulation range $1.6 \leq M_a/M_e \leq 8.0$.

Comparison of theory (eq 11 with $\Gamma = 1$) and simulation (eq 18) for the cubic lattice matrix is shown in Figure 1. The results differ considerably through the range actually covered by the simulations, but they appear to converge as $M_a/M_e$ increases beyond that range. The theory for $\Gamma = 1$ agrees rather well with the continuation of eq 18 out to quite large values of $M_a/M_e$ (the range covered by our self-diffusion results), but the extrapolation is rather long, so that the agreement may well be fortuitous.

The tracer diffusion coefficients for three-arm HPB stars in linear polyethylene show clear evidence of a matrix effect beyond $M_a \sim 9.0 \times 10^3$.[3] For the smaller stars in that study ($1.0 \times 10^3 \leq M_a \leq 7.5 \times 10^3$) $D_B$ decreases in a roughly exponential fashion with increasing $M_a$, and we assume those results reflect the fixed matrix behavior. The reported least-squares fits of linear and star HPB data at 176 °C, when combined with $M_e = 1.25 \times 10^3$ for HPB,[23] give the expression

$$D_B/D_L = 0.0705(M_a/M_e)^{0.95} \exp[-0.76M_a/M_e] \quad (19)$$

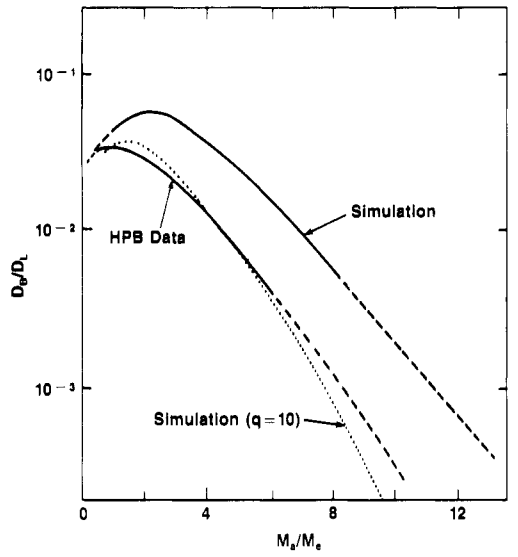


**Figure 2.** Comparison of computer simulation and experimental data on hydrogenated polybutadiene in the fixed-matrix range. Computer data (eq 18) and the experimental results (eq 19) are shown as solid lines over the ranges they cover and as dashed lines outside those ranges. The dotted line represents eq 18 after adjustment to $q = 10$ with eq 20.

for the range $0.8 \leq M_a/M_e \leq 6.1$. This correlation, based on an assumed $M_a^{-1}$ prefactor for stars, will change somewhat with temperature owing to differences in temperature coefficients of $D_L$ and $D_B$[3] and their variation with $M_a$ in the latter (see below).

Comparison of eq 19 with the simulation data (eq 18) is shown in Figure 2. The values from simulation are larger by factors of 1.3–4.0 where the ranges overlap, and they decrease slightly less rapidly with $M_a/M_e$. In the theoretical expression (eq 11 and 12) the choice of lattice number $q$ affects primarily the exponential coefficient. On that basis, the simulation results can be "adjusted" to $q$ values other than 6

$$(D_B/D_L)_q = (D_B/D_L)_6 \exp[[\gamma(6) - \gamma(q)]M_a/M_e] \quad (20)$$

where $\gamma(q)$ is given by eq 12. The simulation results, adjusted in this way to $q = 10$, fit the experimental data rather well (Figure 2), but they then extrapolate quite differently to large values of $M_a/M_e$.

Thus, although theory, simulation, and experiment give comparable results for $D_B/D_L$ vs. $M_a/M_e$ in fixed matrices, the range of $M_a/M_e$ is too small (for simulation and experiment), and the agreement too tenuous, to establish a convincing extrapolation formula. Lacking this, we will use the expression correlating experimental data for HPB (eq 19) to provide the fixed matrix base line for interpreting our self-diffusion results.

**Self-Diffusion and Viscoelasticity.** Any self-diffusion coefficient can be expressed in terms of microscopic events by the formula

$$D = \Delta^2/6\tau \quad (21)$$

where $\tau$ is a mean time between randomly directed displacements of the molecular center of gravity and $\Delta^2$ is the mean-square displacement corresponding to that time. Consider now an entangled liquid of monodisperse polymers from the point of view of the tube model, and suppose for the moment that the effect of constraint release is negligible.[25] If a small step strain is imposed on the liquid, the time for final stress relaxation corresponds directly with the final abandonment of the original tubes. That time can be estimated from the viscoelastic properties of the liquid[26]

$$\tau = \eta_0 J_e^0 \quad (22)$$

where $\eta_0$ is the zero-shear viscosity and $J_e^0$ is the steady-state recoverable shear compliance. Linear chains, moving by reptation, translate a distance of the order of the radius of gyration $R_G$ during that time, so $\Delta^2 \sim R_G^2$. Three-arm stars, moving by arm retraction, translate a much smaller distance, of the order of the mesh size, so $\Delta^2 \sim a^2$. Thus we expect

$$D_L \sim R_G^2/6(\eta_0 J_e^0)_L \quad (23)$$

$$D_B \sim a^2/6(\eta_0 J_e^0)_B \quad (24)$$

Equation 23 becomes an exact result of the Doi–Edwards theory for linear chains if the right-hand side is multiplied by $^6/_5$.[12]

Experimentally, $J_e^0 \sim 2.5/G_N^0$ for nearly monodisperse linear polymers,[27] and $J_e^0 \sim 0.6M_a/\rho RT$ for stars.[21] The mesh size can be estimated with the Doi–Edwards equation for primitive path step length[12]

$$a^2 = {}^4/_5(\langle r^2\rangle/M)\, M_e \quad (25)$$

when $\langle r^2\rangle/M$ is the ratio of the mean-square end-to-end distance to molecular weight for linear chains of the species. Combining results, we arrive at the following approximate relationships between observables for linear polymers and three-arm stars:

$$(\eta_0 D)_L = 0.011\rho RT(\langle r^2\rangle/M)\, M/M_e \quad (26)$$

$$(\eta_0 D)_B = 0.22\rho RT(\langle r^2\rangle/M)\, (M_a/M_e)^{-1} \quad (27)$$

If the tube model is a valid way to view the problem, the equation for stars should apply either when constraint release effects are negligible or when they reduce viscosity and increase diffusion by the same factor.

**Constraint Release Contributions in Star Polymer Diffusion.** We assume that the constraint release development in ref 22 is adequate for dealing with matrix contributions to star polymer mobility. Accordingly

$$D = D_0 + D_{CR} \quad (28)$$

where $D_0$ is the diffusion coefficient in a fixed matrix and $D_{CR}$ is the contribution from path migration due to finite constraint lifetimes. The latter depends on $\tau_w$, the mean waiting time for constraint release. The idea is that each path step of a diffusant polymer is defined by a certain number $z$ of constraints supplied by path steps of the matrix polymer and that the primitive path of the diffusant can jump locally by a distance of the order of the mesh size whenever one of the $z$ steps is abandoned. When the matrix effect dominates, the diffusant migrates in Rouse-like fashion (random local hops of distance $a$), and

$$D_{CR} = a^2/12N\tau_w(z) \quad (29)$$

where $N$ refers to diffusant and $\tau_w(z)$ to matrix. For monodisperse matrices

$$\tau_w(z) = \int_0^\infty [f(t)]^z\, dt \quad (30)$$

where $f(t)$ is the fraction of initial path for the matrix polymer that is still occupied after time $t$. For a star polymer matrix, moving only by arm retraction[22]

$$\tau_w(z) = [S_3(z)/zN_a{}^z P_0(N_a)](\tau_e)_B \quad (31)$$

where $N_a$ is the number of primitive path steps per arm ($N_a = N/3$) and $S_3(z)$ is a summation of terms that is insensitive to $z$ and of order unity.[22]

Equations 28–30 provide a reasonable account of diffusion behavior in linear chain melts,[9] but some modification is required for stars. For linear chains, moving by repta-

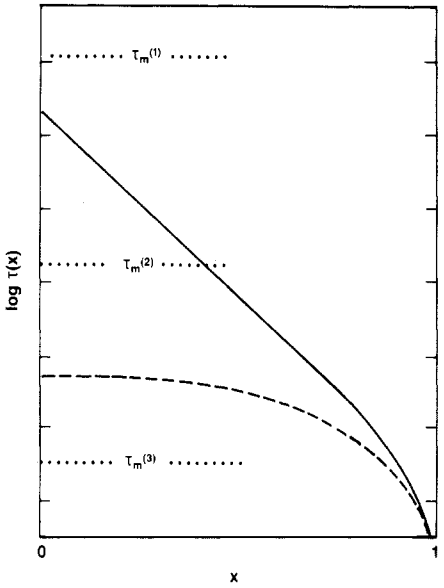


**Figure 3.** Lifetime of path steps vs. molecular location for linear chains and stars. Fractional chain distance from center to free end is denoted by $x$. The nearly constant lifetime for linear chains relaxing by reptation alone is indicated by the dashed line: $\tau(x) \sim \tau_d \cos(x/2)$ (obtained from eq 6 of ref 22). The roughly exponential decrease with $x$ for stars relaxing by arm retraction alone is indicated by the solid line. Three matrix lifetimes (corresponding to $\tau_w$ in the model) are shown where diffusion of a star is dominated by (1) arm retraction alone, (2) constraint release with $\lambda < N_a$ in eq 32, and (3) constraint release with $\lambda \sim N_a$ in eq 32. Diffusion by linear chains is dominated by reptation in all three cases as long as $\tau_d \ll (\tau_m/N^2)(\tau_d/N^2)$.

tion, the lifetime of path steps is not very sensitive to their location along the chain. Thus, $D_0$ dominates when $\tau_w$ is somewhat larger than $\tau_d/N^2$ for the diffusant, $D_{CR}$ dominates when $\tau_w$ is somewhat smaller, and the crossover region is fairly narrow. However, for star polymer diffusants the step lifetimes are governed by partial arm retraction. As a result, they vary enormously with chain location, decreasing in a roughly exponential manner with distance from the branch point. The situation is sketched in Figure 3. Beginning at the fixed matrix limit, hopping starts to contribute as $\tau_w$ approaches the branch point lifetime $\sim(\tau_e)_B/P_0$, but in that regime $D_{CR} \sim a^2/12\tau_w$ applies instead of eq 29 because branch-point mobility still controls the diffusion rate. As $\tau_w$ decreases, the domain where hopping is significant gradually expands. Local hopping finally dominates the mobility in all parts of the star, and eq 29 applies only when $\tau_w$ is smaller than $(\tau_e)/P_0$ by an exponential function of the arm length. Thus, for three-arm stars, we write

$$D_{CR} = \frac{a^2}{12\tau_w\lambda} \tag{32}$$

where $\lambda \sim 1$ for $\tau_w \gtrsim (\tau_e)_B/P_0$ and $\lambda \sim N = 3N_a$ for $\tau_w \ll (\tau_e)_B/P_0$, with a crossover regime that grows exponentially with diffusant arm length. We will treat $\lambda$ as a constant in our data analysis (see Appendix for estimates of $\lambda$ in self-diffusion and some justification for assuming that $\lambda$ is insensitive to $N_a$ in self-diffusion).

Using eq 31 and 32 together with the expression in eq 4 for the diffusion coefficient of stars in a fixed matrix, we arrive at the following result for self-diffusion in stars:

$$D_{CR} = (zN_a^z/6\lambda S_3\Gamma)D_0 \tag{33}$$

where the values of $\lambda$ ($1 \le \lambda \le N$) are in principle unknown. A variety of evidence, including recent studies of viscoelasticity in polybutadiene mixtures,[28] polystyrene mixtures,[29] and tracer diffusion in polystyrene,[9] suggest values of $z$ in the range 3–3.5. For $z = 3$, and with eq 7 and 33

$$D_{CR} = (0.98/\lambda S_3\Gamma)\left(\frac{M_a}{M_e}\right)^3 D_0 \tag{34}$$

This relationship implies a very large contribution from constraint release for the stars in the present study ($6 \le M_a/M_e \le 26$) unless the combination $\lambda S_3\Gamma$ happens to be very large compared to unity. The exponential portion of the dependence on arm length should be the same for self-diffusion and for tracer diffusion in a fixed matrix. The prefactor, however, should be larger for self-diffusion, and that disparity in magnitudes should grow with some modest power of $M_a/M_e$. This contrasts sharply with the linear chain case, where the matrix contribution to self-diffusion should diminish with increasing chain length.

**Table I**
**Molecular Weights of Three-Arm Star Polybutadienes**

| sample | $\bar{M}_n \times 10^{-4}$ | $\bar{M}_w \times 10^{-4}$ |
|---|---|---|
| PB22[a] | $2.0_9$ | $2.1_9$ |
| PB47 | $4.3_3$ | $4.6_5$ |
| PB60[b] | | $6.0_0$ |
| PB71 | $6.8_6$ | $7.1_0$ |
| PB72[b] | | $7.2_0$ |
| PB95 | $9.4_1$ | $9.5_0$ |
| PB144 | 13.8 | 14.4 |

[a] This sample was also used by Klein et al.[3] and was designated WG-1A in that work. [b] Unfractionated stars.

## Experimental Section

**Characterization.** The polymers were prepared from three-arm star polybutadienes (PB) by the catalytic addition of hydrogen to form HPB or deuterium to form DPB. These fully saturated materials have the same chemical microstructure as the linear diffusants in our previous study.[10] They closely resemble polyethylene in melt-state properties and have the advantage of narrow molecular weight distribution. They contain ~20 ethyl branches per $10^3$ main chain carbon atoms, derived from vinyl groups in the precursor polybutadienes (~8% 1,2 addition in the polymerization).

Butadiene was polymerized anionically with *sec*-butyllithium as the initiator and methyltrichlorosilane as the linking agent. Five samples were made in benzene at room temperature under vacuum-line conditions. Linking was carried out with active centers in 10–20% excess relative to the chlorosilane to avoid the presence of linear "doublet" chains in the product. The unlinked arms were removed by fractionation. Two other samples (PB60 and PB72) were made in cyclohexane at 50 °C under argon.[30] Linking was carried out as near to stoichiometry as possible. These products were not fractionated.

Molecular characterization of the polybutadiene samples was done by a combination of size exclusion chromatography (SEC) (Waters 150C), osmometry (Wescan 231), and low-angle laser light scattering (LALLS) (Chromatix KMX-6). The distributions are narrow, as shown by the results in Table I. Number-average molecular weights of unlinked arm and fractionated star demonstrated that, within experimental error, the desired functionality of three was achieved. Figure 4 shows representative SEC results for fractionated and unfractionated star polybutadienes.

The stars were hydrogenated and deuterated to form matched pairs, as described previously.[10] Infrared analysis showed that saturation via $Pd/CaCO_3$ catalysis was virtually complete in all cases.

The molecular weights for HPB and DPB used in the subsequent analyses of data were calculated from the LALLS molecular weights of the polybutadiene stars, taking into account the small changes brought about by hydrogenation and deuteration.[10] The saturated polymers were also evaluated by Dr. G. VerStrate of Exxon Chemical Co. via a Chromatix KMX-6 photometer on line with a Waters 150C SEC at 135 °C.[31] Supplemental character-

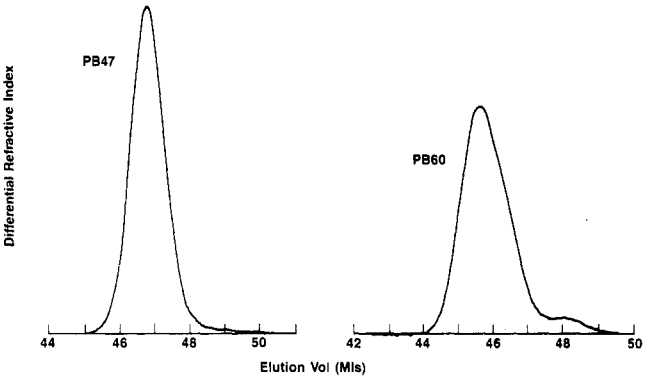


**Figure 4.** Size exclusion chromatographs for polybutadiene stars. Sample PB47 was prepared by vacuum-line techniques and fractionated to remove unlinked arms. Sample PB60 was prepared under argon and not fractionated. The satellite peak for PB60 is unlinked arm. The SEC width at half-height for PB60 is larger by ~30% than that for PB47, strongly suggesting the presence of linear doublet as well.

**Table II**
**Rheological Properties of Star-Branched Hydrogenated Polybutadienes**

| sample | temp, °C | $\eta_0$, P | $E_V$[a] kJ/mol |
|---|---|---|---|
| HPB22 | 115 | $3.90 \times 10^2$ | |
| | 145 | $1.82 \times 10^2$ | 37 |
| | 165 | $1.05 \times 10^2$ | |
| DPB47 | 125 | $1.07 \times 10^4$ | |
| | 165 | $3.09 \times 10^3$ | 43 |
| | 190 | $1.82 \times 10^3$ | |
| HPB71 | 125 | $6.61 \times 10^5$ | 48 |
| | 165 | $1.78 \times 10^5$ | |
| HPB95 | 125 | $1.18 \times 10^7$ | 63 |
| | 165 | $2.11 \times 10^6$ | |

[a] For linear HPB, $E_V$ = 7.2 kcal/mol = 30 kJ/mol.

ization was also done with dilute solution viscosities in trichlorobenzene at 135 °C.[31] Those results were in essential agreement with molecular weights calculated from the data in Table I. The SEC/LALLS measurements on the saturated products from fractionated PB stars also revealed the presence of uncoupled arms (~5%). This appears to be due to a small amount of degradation involving the Si–C bonds at the star center. A correspondingly larger amount (~15%) was found in the products from the unfractionated PB stars. The latter probably contain linear doublets as well as unlinked arms.[31]

The final melting temperatures of the HPB and DPB stars ranged from 101 to 109 °C with $T_m$ for each DPB being about 2 °C less than that of the corresponding HPB. The deuterium fraction in the DPB stars ranged from 0.39 to 0.46.[31,32]

The rheological properties of selected HPB and DPB samples were measured with a Rheometrics mechanical spectrometer. The dynamic moduli, $G'(\omega)$ and $G''(\omega)$, were determined as functions of frequency at various temperatures; values of zero-shear viscosity $\eta_0$ and flow activation energy $E_v$ were obtained by procedures described elsewhere.[31,34] The data for linear samples agreed well with earlier results for HPB[33,34] with no detectable difference between the members of matched HPB/DPB pairs.[31] The data obtained for star samples are given in Table II. The progressive increase in $E_v$ with arm length is consistent with observations reported earlier for similar HPB stars.[32,33] We believe the $\eta_0$ vs. $M_a$ relationship obtained here is more reliable, however, owing to a better definition of molecular weights and fractionation of the PB precursors.

**Diffusion.** Compositionally modulated films for the diffusion experiment were prepared by successive solution casting as described previously.[10] The films consist of alternating layers of matched HPB and DPB with a layer thickness of the order of microns. The solution-casting procedure was not satisfactory for the matched pair of lowest molecular weight, HPB22/DPB22, because of mechanical problems (peeling and cracking). For that case, thin sheets of the individual components were compression-molded, cut into disks with a cork borer, and stacked alternately to fill a Teflon cylinder of the same diameter. Thin brass plates were then bolted on top and bottom to prevent flow during the heating cycle.

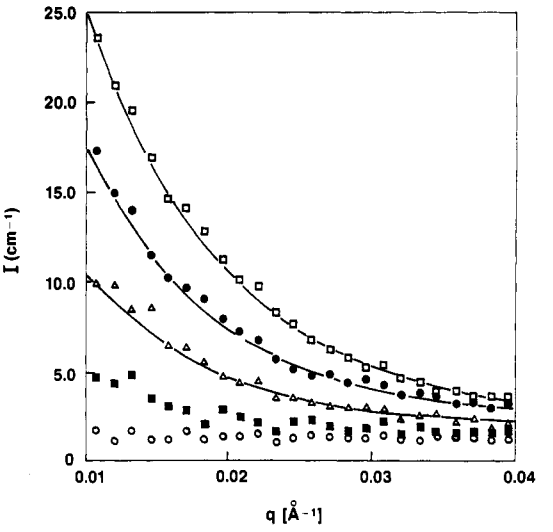


**Figure 5.** Small-angle neutron scattering patterns for the HPB71/DPB71 films. The symbols denote the as-formed layered film (■), the film after total diffusion times of 2.2 h (△), and 8.2 h (●) at 165 °C, a solution blend representing $t = \infty$ (□), and pure HPB71 (○). The solid lines are rescaled plots (above a constant base line) of the single particle scattering function for three-arm stars with $R_G$ = 139 Å, the radius of gyration for HPB71.[32]

Diffusion coefficients were obtained from the changes in the small-angle neutron scattering pattern that result from partial homogenization when the films are held for a known time in the melt state. All scattering patterns were recorded on samples that had been quenched to room temperature to arrest the diffusion process. The SANS measurements were made in the 10-m facility of the Oak Ridge National Laboratory using a sample-to-detector distance of 4.5 m and neutron wavelength λ 4.75 Å. Intensities were obtained for a range of scattering vectors, $0.01 \leq q \leq 0.12$ Å$^{-1}$; partial homogenization was accomplished and the scattering data were worked up as described previously.[10] Diffusion times ranged from 10 min to 71 h. Most data were gathered for a melt temperature of 165 °C, but other temperatures were used occasionally to establish temperature dependencies.

The first experiments were conducted with stars from the unfractionated PB precursors. The presence of rapidly diffusing species, unlinked arms and linear doublets, was apparent from the rapid increase in SANS intensity at short times (~minutes), followed by a much slower drift toward full homogenization at longer times (~hours). Subsequent experiments were conducted with the stars from fractionated precursors. Contributions from unlinked arms were practically undetectable in those cases; the analysis to obtain $D$ was straightforward.[10]

Figure 5 shows the SANS patterns for a typical fractionated star system, HPB71/DPB71, after diffusion times of 2.2 and 8.2 h at 165 °C. Also shown are scattering patterns for the as-prepared film ($t = 0$), a 50–50 solution blend (representing $t = \infty$), and pure HPB (representing an ideally nonmixed layered film). It can be seen that a small amount of HPB/DPB mixing exists in the as-prepared film. This was most noticeable in films whose layer thickness was less than 5 μm and was taken into account when calculating $D$.[10] Diffusion coefficients, obtained from the increase in intensity at constant $q$, were independent of $q$ (±5%) and are reported in Table III. The activation energy $E_{D/T}$[10] was also determined for two samples. These values are subject to considerable uncertainty. Like $E_v$, the values of $E_{D/T}$ are clearly larger than those for linear chains, $E_{D/T}$ = 23 kJ/mol,[10] and they appear to increase with arm length. At this time, however, we do not believe that the differences between $E_V$ and $E_{D/T}$ for self-diffusion, 43 vs. 38 kJ/mol for HPB47 and 48 vs. 60 kJ/mol for HPB71, are experimentally significant. Elevated activation energies have also been observed in HPB stars diffusing in a linear polyethylene matrix.[3]

**Table III**
**Diffusion Data for Three-Arm Star Hydrogenated Polybutadienes**

| sample | $M \times 10^{-4}$ [a] | $T$, °C | $L$, μm | $D$,[b] cm²/s | $E_{D/T}$, kJ/mol |
|---|---|---|---|---|---|
| | | Fractionated Precursor | | | |
| HPB22/DPB22 | 2.3 | 165 | 87 | $1.3 \times 10^{-9}$, $7.8 \times 10^{-10}$ | |
| | | 165 | 83 | $8.4 \times 10^{-10}$ | |
| HPB47/DPB47 | 4.8 | 125 | 9.9 | $6.1 \times 10^{-12}$, $4.6 \times 10^{-12}$ | 38 |
| | | 145 | 10.4 | $8.9 \times 10^{-12}$ | |
| | | 165 | 12.5 | $1.5 \times 10^{-11}$, $1.8 \times 10^{-11}$ | |
| HPB71/DPB71 | 7.4 | 125 | 1.8 | $2.4 \times 10^{-14}$ | 60 |
| | | 165 | 3.1 | $1.4 \times 10^{-13}$, $1.4 \times 10^{-13}$ | |
| HPB95/DPB95 | 9.9 | 165 | 1.2 | $7.9 \times 10^{-15}$ | |
| HPB144/DPB144 | 14.9 | 165 | 0.6 | $<10^{-16}$ | |
| | | Unfractionated Precursor | | | |
| HPB60/DPB60 | 6.2 | 165 | 8.4 | $1.6 \times 10^{-12}$ | |
| HPB72/DPB72 | 7.5 | 165 | 8.0 | $1.3 \times 10^{-13}$ | |

[a] Rounded values of molecular weight for the HPB component, obtained by multiplying the $\bar{M}_w$ value for PB in Table I by 56/54 and used in subsequent figures and discussions. Values of $M_a$ are $M/3$; values of $M_a/M_e$ are $M_a/1250$. [b] Multiple values of $D$ on the same line are diffusion coefficients for successively longer diffusion times with the same layered film. Values on different lines were obtained with different films.

The star of highest molecular weight, HPB144/DPB144, showed no detectable change in SANS pattern after 71 h at 165 °C relative to the pattern obtained after a 10-min anneal at the same temperature. On this basis and considering the experimental uncertainties, the upper bound on diffusion coefficient for this polymer is $10^{-16}$ cm²/s. (A similar "null" result was obtained for the diffusion coefficient of linear HPB ($\bar{M}_w = 7.3 \times 10^4$) at 95 °C, 14 °C below its final melting temperature.[31] The upper bound in that case was $5 \times 10^{-14}$ cm²/s, much smaller than the extrapolated melt-state value of $2.5 \times 10^{-11}$ cm²/s.)

Diffusion coefficients for the stars from unfractionated precursors (HPB60 and HPB72) were estimated from changes in intensity between the first and second diffusion times. This procedure should be valid if the diffusion coefficients of the minor fast components (~15% linear chain contaminants) and major slow component (~85% star polymer) are sufficiently different, which is the situation here. The values of $D$ obtained by this procedure (Table III) agreed within ±10% above $q = 0.016$. These values are of course not quite the same as self-diffusion coefficients, owing to the linear chain contamination, so we do not place strong reliance on them in the interpretation. However, the agreement between HPB71/DPB71 (fractionated precursor) and HPB72/DPB72 (unfractionated precursor), which have nearly the same molecular weight, suggests that the contaminant effect is not very important.

## Results and Discussion

The self-diffusion coefficients for three-arm HPB stars at 165 °C are shown in Figure 6. Averages were used when more than one value was available except for the lowest molecular weight sample, where the spread of independent estimates was largest. The solid line represents the results for linear HPB ($D_L \propto M^{-2}$), shifted from 125 to 165 °C with the observed activation energy, $E_{D/T} = 23$ kJ/mol.[10] It is evident that the stars diffuse more slowly than linear chains of the same molecular weight and that $D$ vs. $M$ for stars is not described by a power law. The data in fact conform rather well to an exponential dependence, as shown by Figure 7. The best fit to a simple exponential is (for $M_e = 1.25 \times 10^3$ and $M_a = M/3$)

$$D \propto \exp(-0.59 M_a/M_e) \quad (35)$$

Extrapolation to $M = 1.47 \times 10^5$ gives $D \sim 10^{-19}$ cm²/s for HPB144/DPB144, which is certainly consistent with undetectability of movement ($D < 10^{-16}$ cm²/s), as observed.

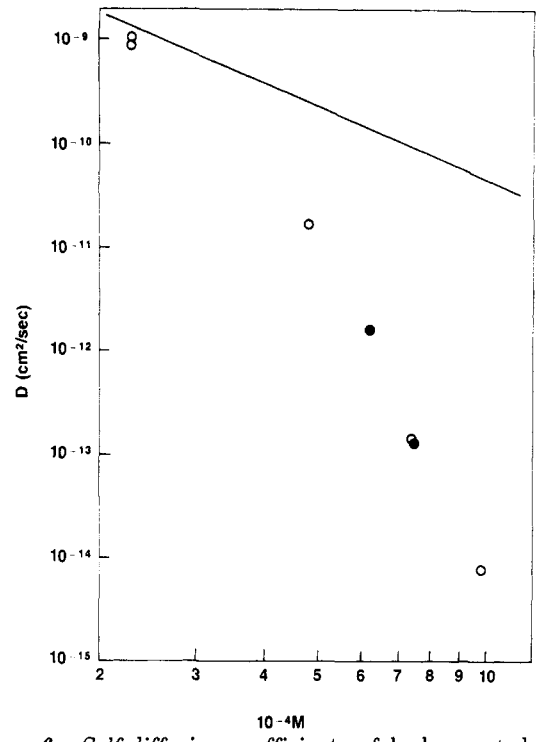


**Figure 6.** Self-diffusion coefficients of hydrogenated polybutadiene three-arm stars at 165 °C. The values obtained with unfractionated samples are indicated by filled circles. The solid line represents the self-diffusion data at 165 °C for linear HPB.[10]

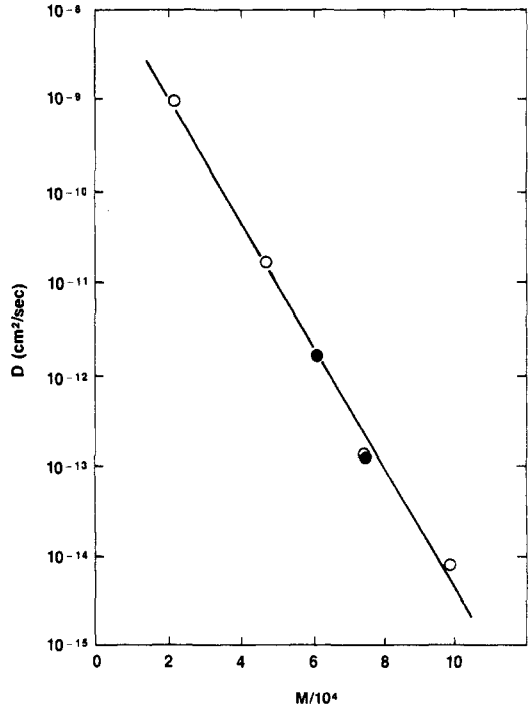


**Figure 7.** Test of exponential dependence on molecular weight for the self-diffusion coefficients of stars.

We have explored the possible effect of a preexponential power of molecular weight with these data ($A_1 \propto M_a^p$ in eq 2). Correlation coefficients were determined for log $(D/M_a^p)$ vs. $M_a/M_e$ with various integer values of $p$. The correlation coefficient was greater than 0.99 for $-1 \leq p \leq 2$ and decreased appreciably outside that range. Even within the range, the exponential coefficient changed with $p$, being 0.73 for $p = 2$, for example, as opposed to 0.59 for $p = 0$. Thus, the exponential form seems certain from

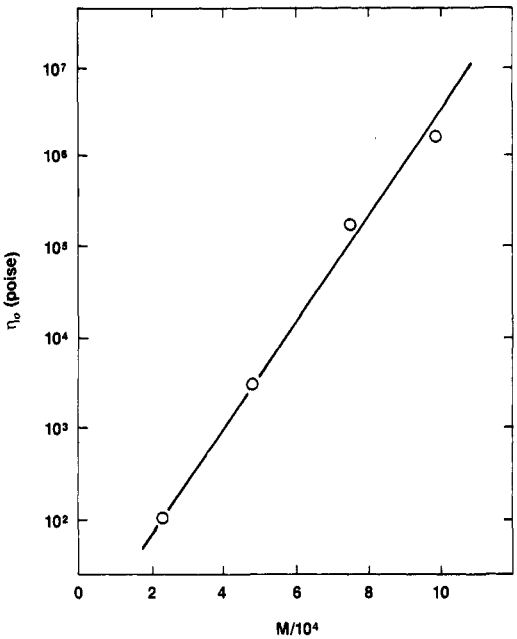


**Figure 8.** Test of exponential dependence on weight for the viscosity of stars.

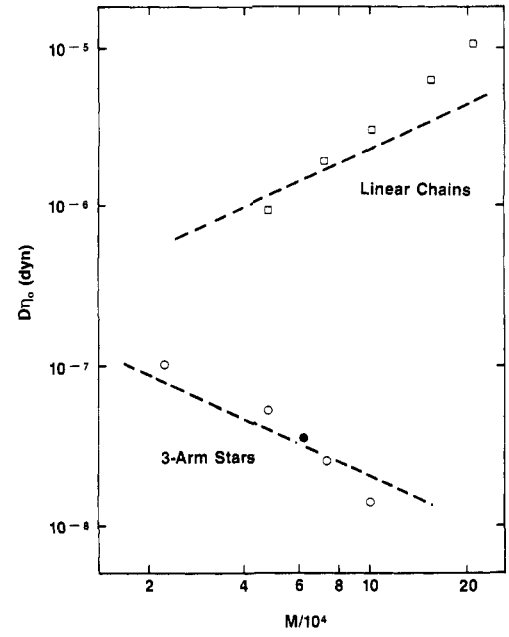


**Figure 9.** Comparison of tube model predictions for $\eta_0 D$ in linear and three-arm star polymers. The filled symbol represents an unfractionated star (HPB60) with $\eta_0$ obtained by interpolation in Figure 8. The dashed lines are the predictions from eq 26 and 27.

these data, but it so overwhelms the behavior that the preexponential power dependence cannot be established with confidence.

Melt viscosities at 165 °C for the stars from fractionated precursors are shown in Figure 8. An exponential dependence on molecular weight is supported reasonably well by these data although with a somewhat different magnitude of exponential coefficient than $D$

$$\eta_0 \propto \exp(0.51 M_a/M_e) \tag{36}$$

However, judged by the previous examination of $D$ vs. $M_a$, that difference might simply reflect different preexponential powers of $M_a$ for $\eta_0$ and $D$.

The product of viscosity and diffusion coefficient at 165 °C is plotted in Figure 9 as a function of molecular weight for linear and star HPB samples. The dashed lines are the predictions of eq 26 and 27 with data for linear polyethylene.[12] The prediction of magnitudes is certainly correct, and it is gratifying to find such a clear distinction between the dynamics of linear chains and stars. For linear HPB the variation with molecular weight, $\eta_0 D \propto M^{1.4}$ is slightly stronger than predicted, reflecting a larger viscosity exponent ($\eta_0 \propto M^{3.4}$) than the cubic dependence predicted by tube models. A similar trend is shown by the stars, with $\eta_0 D$ appearing to decrease more rapidly than the expected $M^{-1}$. However, the latter departures are not really much larger than the experimental uncertainties.

The self-diffusion coefficients for stars from this study are compared at 176 °C with the tracer diffusion coefficients of Klein, Fletcher, and Fetters[3] ($M_a \leq 7.5 \times 10^3$) in Figure 10. The slight adjustments of self-diffusion coefficients from 165 to 176 °C were made with temperature coefficients based on the viscosity. Also shown is $D_B$ vs. $M$ from the simulation result for stars in a fixed matrix, obtained with eq 18 and

$$D_L = 0.48 M^{-1.95} \tag{37}$$

which is the empirical equation for linear HPB data at 176 °C.[3]

Although the tracer and self-diffusion data cover different ranges of molecular weight, they coincide precisely in one instance: HPB22 and HPB sample WG-1A in ref 3 were derived from the same precursor polybutadiene

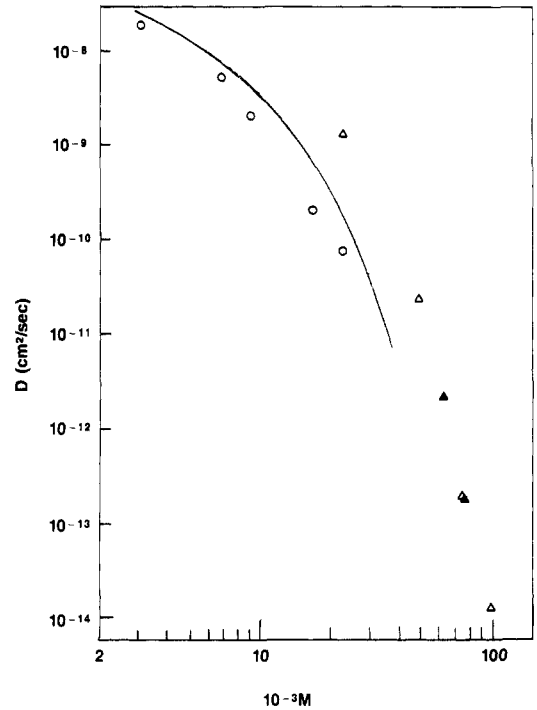


**Figure 10.** Comparison of the tracer diffusion and self-diffusion results for hydrogenated polybutadiene stars at 176 °C. Symbols denote the tracer data of Klein, Fletcher, and Fetters[3] in the range where the matrix effect is negligible (○) and the self-diffusion data of this study, adjusted from 165 to 176 °C (△, ▲). The filled symbols indicated data from the unfractionated stars. The solid line represents the computer simulation result, as explained in the text.

sample. For that sample, ($M = 2.3 \times 10^4$) the self-diffusion coefficient is larger by a factor of about 20. The matrices differ slightly in chemical microstructure, the tracer data having been obtained for a matrix of linear polyethylene. The effect must be small, however, because tracer and self-diffusion coefficients differed by less than 40% for the linear polymers, and tracer diffusion coefficients were

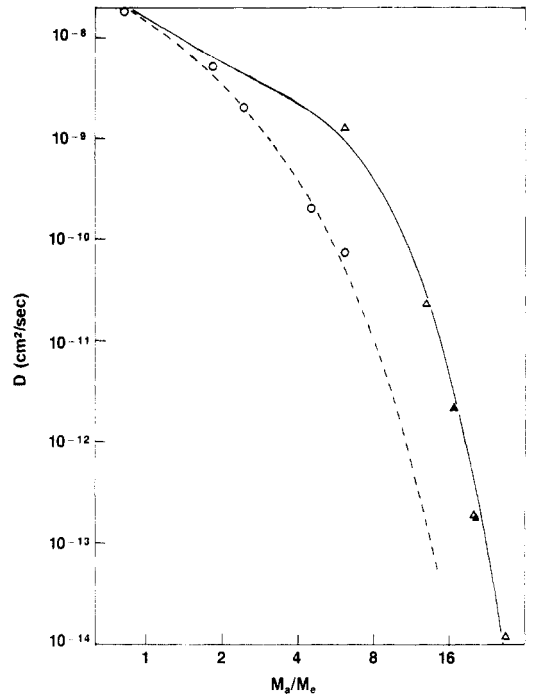


**Figure 11.** Fit of self-diffusion data by the constraint release model. The symbol designations are given in the caption of Figure 10. The dashed line is the fixed matrix base line $D_0(M_a/M_e)$ as obtained from ref 3. The solid line is the result calculated from $D_0$ and eq 38 with $\beta = 0.09$ and $z = 3$.

actually larger in that case.[10] We assume the tracer diffusion data (for $M_a \leq 7.5 \times 10^3$) reflect the fixed-matrix behavior. We conclude that constraint lifetime effects are very important in the self-diffusion of nearly monodisperse entangled star polymers.

It seems justified also to conclude that the relaxation spectrum of stars is strongly modified by constraint release. This follows from the observation that $\eta_0 D$ vs. $M$ (Figure 9) obeys the general tube model form, implying that constraint release reduces $\eta_0$ and increases $D$ by about the same factor. It is also consistent with earlier work by Ferry and co-workers on stress relaxation, where it was shown that stars relax much more rapidly in their own melt than when dilutely dispersed in a network.[35]

Using eq 28 and 33, we can write an expression for the self-diffusion coefficient of stars, including constraint lifetime effects

$$D = [1 + \beta(z)(M_a/M_e)^z]\, D_0 \tag{38}$$

where $D_0$ is the diffusion coefficient in a fixed matrix and $\beta(z)$ is a model-dependent coefficient

$$\beta(z) = z(5/4)^z/6\lambda S_3(z)\Gamma \tag{39}$$

For data-fitting purposes we assume $\beta(z)$ is insensitive to molecular weight (see Appendix) and treat it as a separately adjustable parameter. Using the tracer diffusion expression[3] as an extrapolation formula for $D_0$ (combination of eq 19 and 37), we can now test the fit of eq 38 to the self-diffusion data. Figure 11 shows the result obtained for $\beta = 0.09$ and $z = 3$. This choice of $\beta$ is in fact within a factor of 3 or so of the estimate, $\beta(z) \sim 0.025$–$0.04$ for $z = 3$, given in the Appendix. Values of $z$ between 2.5 and 3.5 with $\beta$ adjusted accordingly give about the same fit. The agreement is reasonable, and the range of $z$ is the consistent with estimates from the other experiments.[9,28,29]

Unfortunately, the comparisons for most of the stars are based on a long and uncertain extrapolation to establish values of $D_0$. The variation of temperature coefficients with arm length for HPB adds another complication, since the relative values of $D$ would be somewhat different at another temperature. As a result, conclusions about agreement with particular models for the constraint release contribution must be regarded as tentative.

## Summary and Conclusions

Self-diffusion coefficients have been measured for a series of three-arm star hydrogenated polybutadienes in the melt state at 165 °C and at a few other temperatures for selected samples to determine activation energies. Melt viscosities were also measured; both $\eta_0$ and $D$ were found to be exponential functions of the arm molecular weight. The results, together with published data on tracer diffusion coefficients in a matrix of high molecular weight linear polyethylene, were used to test molecular theories of entangled chain dynamics based on the tube model. In contrast with earlier results for linear polymers, the self-diffusion of stars is much faster than tracer diffusion when the latter takes place in an effectively immobile matrix. The difference was explained in terms of constraint release, a mechanism that dominates self-diffusion for entangled stars but has little effect for correspondingly entangled linear polymers. Comparisons with the viscosity data suggest that constraint release is equally important in the low-frequency mechanical response of entangled star melts.

**Acknowledgment.** The SANS measurements were accomplished with the advice and assistance of Dr. George Wignall at the Oak Ridge National Laboratory. We are grateful to Dr. Gary VerStrate of Exxon Chemical Co. for supplemental characterization of the hydrogenated polymers. Discussions with Dr. D. S. Pearson and Dr. J. Klein, leading to eq 26 and 27, were extremely valuable. We are also grateful to Dr. Klein for pointing out an important error in the manuscript. The work was supported by the Northwestern University Materials Research Center (NSF/MRL Program Grant DMR-82-16972), by a grant from Exxon Chemical Co., and by a fellowship from IBM Corporation (C.R.B.).

## Appendix

Consider a well-entangled three-arm star diffusant ($N_a \gg 1$) and label the primitive path steps of each arm 0, 1, 2, ---, $n$, ---, beginning at the junction. In a fixed matrix the mean lifetime of step $n$ is governed by fluctuations in path length. We assume it can be written

$$\tau_n(N_a) = (\tau_e)_B/P_n(N_a) \tag{A-1}$$

or

$$\tau_n(N_a) = \alpha_n \tau_0(N_a) \tag{A-2}$$

where $\alpha_n = P_0(N_a)/P_n(N_a)$ is the ratio of probabilities for path lengths of 0 and $n$ when the average is $N_a$ and $\tau_0(N_a) = (\tau_e)_B/P_0(N_a)$ is the mean time for full arm retraction. An expression for $\alpha_n$ is readily deduced from the Helfand–Pearson eq 4.9[24] for a regular $q$-lattice matrix. Using eq 6 to convert from chain steps to path steps, we obtain

$$\alpha_n = (1 + n) \exp\left[-\frac{q}{q-2}\frac{\ln(q-1)}{2}n\right] \tag{A-3}$$

In a matrix with finite lifetime the mean hopping time, $2\tau_w$, is the same for all path steps of the diffusant. Consider the situation when the hopping time is somewhat smaller than the full retraction time $\tau_0(N_a)$. Hopping is faster than disengagement by partial retraction for path steps near the junction and slower for the more remote steps. The crossover ($n = n^*$) is located where these times are comparable

$$\tau_{n^*}(N_a) = 2\tau_w \quad \text{(A-4)}$$

The waiting time for constraint release in a matrix of star polymers is given by eq 31, which we now rewrite as

$$\tau_w = (S_3(z)/zN_a^z)\tau_0(N_a) \quad \text{(A-5)}$$

Combining eq A-2, A-4, and A-5, we determine that the crossover for star self-diffusion occurs when the equation

$$\alpha_n^* = 2S_3(z)/zN_a^a \quad \text{(A-6)}$$

is satisfied. This relationship permits evaluation of the parameter $\lambda = 3(1 + n^*)$, which appears in eq 32 for $D_{CR}$. The following table presents $\lambda$ as a function of $N_a$, calculated for $z = 3$ and $S_3(z) \sim 1.5^{22}$ with eq A-5–A-7 with $q = 6$ in eq A-3.

| $N_a$ | $n^*$ | $\lambda$ |
|---|---|---|
| 3.2 | 2 | 9 |
| 8.6 | 4 | 15 |
| 21.4 | 6 | 21 |
| 52.1 | 8 | 27 |

The results in this table suggest that $\lambda$ changes rather slowly with branch length over the range covered by our experiments ($7.5 < N_a < 33$, using $N_a = (5/4)M_a/M_e$ from eq 7). Taking the tabulated values literally, as well as $S_3(3) = 1.5$ and $\Gamma = 1$ (from the comparison of simulation and theory in Figure 1), we estimate values of $\beta(z)$ (eq 39) ranging from 0.025 to 0.04 ($z = 3$) for our polymers. Aside from reservations about the correctness of these magnitudes, which clearly rely excessively on model details, the variation of $\beta(z)$ with arm molecular weight is certainly weak compared with the power law and exponential dependences of the other quantities in eq 38. It thus seems sensible to treat $\beta(z)$ as a constant for the purpose fitting data, such as done in Figure 11.

**Registry No.** neutron, 12586-31-1.

## References and Notes


(1) Present address: PO Box 509, Texaco, Inc., Beacon, NY 12508.
(2) Tirrell, M. *Rubber Chem. Technol. Rubber Rev.* **1984**, *57*, 523 (reviews work on polymeric diffusion prior to 1984).
(3) Klein, J.; Fletcher, D.; Fetters, L. J. *Nature (London)* **1983**, *304*, 526; *Faraday Symp. Chem. Soc.* **1983**, *No. 18*, 159.
(4) Bachus, R.; Kimmich, R. *Polymer* **1983**, *24*, 964.
(5) Fleischer, G. *Polym. Bull. (Berlin)* **1983**, *9*, 152.
(6) Von Meerwall, E.; Grigsby, J.; Tomich, D.; Van Antwerp, R. *J. Polym. Sci., Polym. Phys. Ed.* **1982**, *20*, 1037. Von Meerall, E. *Adv. Polym. Sci.* **1984**, *54*, 1.
(7) Antonietti, M.; Coutandin, J.; Grütter, R.; Sillescu, H. *Macromolecules* **1984**, *17*, 798. Antonietti, M.; Sillescu, H. *Macromolecules* **1985**, *18*, 1162.
(8) Smith, B. A.; Samulski, E. T.; Yu, L.-P.; Winnik, M. A. *Phys. Rev. Lett.* **1984**, *52*, 45. Nemoto, N.; Landry, M. R.; Noh, I.; Yu, H. *Polym. Commun.* **1984**, *25*, 141.
(9) Green, P. F.; Mills, P. J.; Palmstrom, C. J.; Mayer, J. W.; Kramer, E. J. *Phys. Rev. Lett.* **1984**, *53*, 2145.
(10) Bartels, C. R.; Crist, B.; Graessley, W. W. *Macromolecules* **1984**, *17*, 2702.
(11) Doi, M.; Edwards, S. F.; *J. Chem. Soc., Faraday Trans. 2* **1978**, *74*, 1789; *Ibid.* **1978**, *74*, 1802.
(12) Graessley, W. W. *J. Polym. Sci., Polym. Phys. Ed.* **1980**, *18*, 27; *Faraday Symp. Chem. Soc.* **1983**, *No. 18*, 7.
(13) Evans, K. E.; Edwards, S. F. *J. Chem. Soc., Faraday Trans. 2* **1981**, *77*, 1891, 1913, 1927.
(14) Kremer, K. *Macromolecules* **1983**, *16*, 1632.
(15) Deutsch, J. M. *Phys. Rev. Lett.* **1982**, *49*, 926; *Ibid.* **1983**, *51*, 1924.
(16) Baumgärtner, A.; Kremer, K.; Binder, K. *Faraday Symp. Chem. Soc.* **1983**, *No. 18*, 37.
(17) Baumgärtner, A. *J. Polym. Sci., Polym. Symp.*, in press.
(18) de Gennes, P.-G. *J. Phys. (Les Ulis, Fr.)* **1975**, *36*, 1199.
(19) Needs, R. J.; Edwards, S. F. *Macromolecules* **1983**, *16*, 1492.
(20) Graessley, W. W. *Acc. Chem. Res.* **1977**, *10*, 332.
(21) Pearson, D. S.; Helfand, E. *Macromolecules* **1984**, *17*, 888.
(22) Graessley, W. S. *Adv. Polym. Sci.* **1982**, *47*, 67.
(23) Ferry, J. D. "Viscoelastic Properties of Polymers"; 3rd ed.; Wiley: New York, 1980.
(24) Helfand, E.; Pearson, D. S. *J. Chem. Phys.* **1983**, *79*, 2054. The divergence at $q = 2$ in eq 3.22 is an artifact of the approximation scheme that was used to express the exact eq 3.21 at large $N$.
(25) This development was suggested to the authors by D. S. Pearson, arising from a discussion with J. Klein. An expression equivalent to eq 27 had been obtained by one of the authors (see eq 2.29 in ref 31 below) based on a less general argument.
(26) Graessley, W. W. *Adv. Polym. Sci.* **1974**, *16*, 1.
(27) Raju, V. R.; Menezes, E. V.; Marin, G.; Graessley, W. W.; Fetters, L. J. *Macromolecules* **1981**, *14*, 1668.
(28) Graessley, W. W.; Struglinski, M. J. submitted for publication. See also the second paper in ref 12.
(29) Montfort, J. P.; Marin, G.; Monge, P. *Macromolecules* **1984**, *17*, 1551.
(30) Rochefort, W. E.; Smith, G. G.; Rachupudy, H.; Raju, V. R.; Graessley, W. W. *J. Polym. Sci., Polym. Phys. Ed.* **1979**, *17*, 1197.
(31) Bartels, C. R. Ph.D. Thesis, Northwestern University, Evanston, IL, 1985.
(32) Tanzer, J. D.; Bartels, C. R.; Crist, B.; Graessley, W. W. *Macromolecules* **1984**, *17*, 2708.
(33) Graessley, W. W.; Raju, V. R. *J. Polym. Sci., Polym. Symp.* **1984**, *No, 71*, 77.
(34) Raju, V. R.; Rachapudy, H.; Graessley, W. W. *J. Polym. Sci., Polym. Phys. Ed.* **1979**, *17*, 1223.
(35) Kan, H.-C.; Ferry, J. D.; Fetters, L. J. *Macromolecules* **1980**, *13*, 1571.


# Diffusion of Linear Polystyrene Molecules in Matrices of Different Molecular Weights


**Markus Antonietti, Jochen Coutandin, and Hans Sillescu***

*Institut für Physikalische Chemie der Universität Mainz, D-6500 Mainz, West Germany.*

*Received July 17, 1985*


ABSTRACT: A holographic grating technique has been used to measure diffusion coefficients $D$ of photolabeled polystyrene (PS) molecules having molecular weights in the range $18\,000 \leq M \leq 100\,000$ in PS matrices of $4000 \leq M' \leq 220\,000$ and a matrix of intra-cross-linked PS ($M' \rightarrow \infty$) at 212 °C. Self-diffusion coefficients ($M = M'$) have been determined in PS and poly(methylstyrene) (PMS), a random copolymer of 60% 3-methylstyrene and 40% 4-methylstyrene ($23\,000 \leq M \leq 425\,000$). A fit to the power law $D \sim M^{-\alpha}$ yields $\alpha$ between 2.4 and 2.5 in a range $30\,000 \lesssim M \lesssim 150\,000$, and $\alpha = 2$ for higher $M$ values. The matrix dependence and the increased $\alpha$ values are explained by considering "tube formation" effects which should influence diffusion in a certain range above the entanglement spacing $M_e$ in the Doi–Edwards reptation model.


## Introduction

Recent studies of polymer-chain diffusion in entangled systems[1-7] have accumulated considerable support for the polymer law $D = D_0M^{-\alpha}$ relating the diffusion coefficient $D$ with the molar mass $M$ by an exponent $\alpha = 2$, as predicted by the reptation model.[8] The same model predicts

0024-9297/86/2219-0793$01.50/0 